particles

MDPI

Article

High-Efficiency WLS Plastic for a Compact Cherenkov Detector

Francesco Nozzoli [1,2,*], Luigi Ernesto Ghezzer [1,2], Francesco Bruni [3,4], Daniele Corti [1], Francesco Meinardi [3], Riccardo Nicolaidis [1,2], Leonardo Ricci [2], Piero Spinnato [1], Enrico Verroi [1] and Paolo Zuccon [1,2]

[1] Istituto Nazionale Fisica Nucleare TIFPA, Via Sommarive 14, I-38123 Trento, Italy
[2] Department of Physics, University of Trento, Via Sommarive 14, I-38123 Trento, Italy
[3] Department of Material Science, Milano Bicocca University, I-20125 Milano, Italy
[4] Glass to Power s.p.a., Via Fortunato Zeni 8, I-38068 Rovereto, Italy
* Correspondence: francesco.nozzoli@unitn.it

Abstract

The Cherenkov effect, whereby a charged particle emits light when traveling faster than the phase velocity of light in a dielectric medium, is widely employed in particle identification techniques. However, Cherenkov light yield is relatively low, typically amounting to only 100–200 visible photons per centimeter of path length in materials like water, plastic, or glass. In this study, we investigate the optical response of FB118, a wavelength-shifting (WLS) plastic developed by Glass to Power, under exposure to ionizing particles. Our measurements confirm the absence of residual scintillation in FB118, allowing for a clean separation of Cherenkov signals. Moreover, the intrinsic WLS properties of the material enable a significant enhancement of light detection in the visible range. These features make FB118 a promising candidate for use in compact Cherenkov detectors, particularly in astroparticle physics experiments where space and power constraints demand efficient, compact solutions.

Keywords: Cherenkov; wavelength shifter; particle identification

Academic Editors: Matteo Duranti and Valerio Vagelli

Received: 20 August 2025
Revised: 7 September 2025
Accepted: 10 September 2025
Published: 12 September 2025

Citation: Nozzoli, F.; Ghezzer, L.E.; Bruni, F.; Corti, D.; Meinardi, F.; Nicolaidis, R.; Ricci, L.; Spinnato, P.; Verroi, E.; Zuccon, P. High-Efficiency WLS Plastic for a Compact Cherenkov Detector. *Particles* **2025**, *8*, 79. https://doi.org/10.3390/particles8030079

1. Introduction

The Cherenkov effect occurs when a charged particle travels through a dielectric medium at a velocity exceeding the speed of light in that medium. This phenomenon leads to the emission of coherent electromagnetic radiation, forming a characteristic light cone. The emission angle θ_C relative to the particle trajectory depends on the particle's velocity $v = \beta c$ and the refractive index η of the medium, as given by

$$\cos\theta_C = \frac{1}{\beta\eta} = \frac{\beta_{\text{thr}}}{\beta}. \tag{1}$$

The spectrum of emitted photons per unit path length, λ, is described by the Frank–Tamm formula:

$$\frac{d^2N}{dx\,d\lambda} = z^2\frac{2\pi\alpha}{\lambda^2}\sin^2\theta_C = z^2\frac{2\pi\alpha}{\lambda^2}\frac{\beta+\beta_{\text{thr}}}{\beta^2}(\beta-\beta_{\text{thr}}), \tag{2}$$

where z is the particle charge. Above the threshold velocity β_{thr}, the number of photons increases almost linearly, and their spectrum is strongly peaked in the ultraviolet (UV) region.

Cherenkov radiation is widely used in many fields. As a non-invasive probe of particle velocity, it enables particle identification in high-energy physics via measurements of the

Cherenkov cone aperture and the number of detected photons. A major limitation, however, is its relatively low light yield: for a relativistic $z = 1$ particle crossing dense media such as water, plastic, or glass, only about 100–200 photons per centimeter are emitted in the visible spectrum. The large fraction of Cherenkov emission in the UV range is typically lost due to self-absorption in the medium and reduced detector efficiency at short wavelengths.

A well-established method to enhance light collection efficiency is to dope water or plastics with wavelength-shifting (WLS) fluors, which convert UV photons to visible light [1,2]. Examples include the use of 1,4-Bis(2-methylstyryl)benzene (bis-MSB) in WLS coatings [3], WLS plate collectors [4], and doped acrylic Cherenkov modules such as those in the SuperTIGER detector [5]. However, the isotropic re-emission typical of WLS materials prevents their use in Ring Imaging Cherenkov (RICH) detectors, where the directional information is essential.

An important characteristic of a Cherenkov radiator is the absence of residual scintillation. Some commercial WLS plastics, such as EJ-286, are known to produce residual scintillation light [6,7].

In the framework of the PHeSCAMI project [8,9], we selected a material produced by "Glass to Power" [10] as a highly efficient WLS material for multi-stage UV conversion [7]. This material, polymethyl methacrylate (MMA) doped with 2,5-Bis(5-tert-butyl-benzoxazol-2-yl)thiophene (BBT, [11]), named FB118, exhibits high UV-to-visible conversion efficiency, making it a promising candidate for high-performance Cherenkov radiators. Preparation details and optical characterization of FB118 are reported in [7].

In this article, we present a characterization of the FB118 response to ionizing radiation. We summarize measurements aimed at determining its Cherenkov light yield and at verifying the absence of residual scintillation, and we discuss its potential applications in compact detectors for astroparticle physics.

2. Test of Scintillation in FB118

We compared the light output of an FB118 sample ($9 \times 4 \times 1$ cm^3) with that of an EJ-200 plastic scintillator of identical dimensions. Two test setups were employed: one for charged particles and one for gamma rays. In both configurations, the samples were optically coupled to the same Hamamatsu R5946 photomultiplier tube (PMT).

The charged particle setup (Figure 1A) consisted of a telescope of two EJ-200 scintillators (Trigger1 and Trigger2) used to tag atmospheric muons traversing the FB118 or EJ-200 sample avoiding the readout PMT. The same configuration was used at the Trento Proton Therapy Center with a proton beam (74–225 MeV) perpendicularly aligned to the center of Trigger1 and Trigger2. Since the setup was externally triggered, no amplitude threshold was applied to the signals from the FB118 or EJ-200 samples.

Figure 2 (top) shows that the EJ-200 response to muons and protons follows expectations from the Bethe–Bloch formula: the energy deposition increases for slower particles.

In contrast, FB118 data (bottom) show negligible signals for protons, indicating no significant scintillation response. This confirms that FB118 light output is dominated by Cherenkov radiation, whose threshold for protons in FB118 ($\eta \simeq 1.5$) is about 320 MeV. Table 1 lists the most probable values (MPVs) of signal amplitudes under the different test conditions.

The light-yield ratio between EJ-200 and FB118 for muons is $9.1 \pm 0.6^{(\text{stat.})} \pm 2.5^{(\text{syst.})}$, with systematic uncertainties derived from variations in PMTs, bias voltages, and optical couplings.

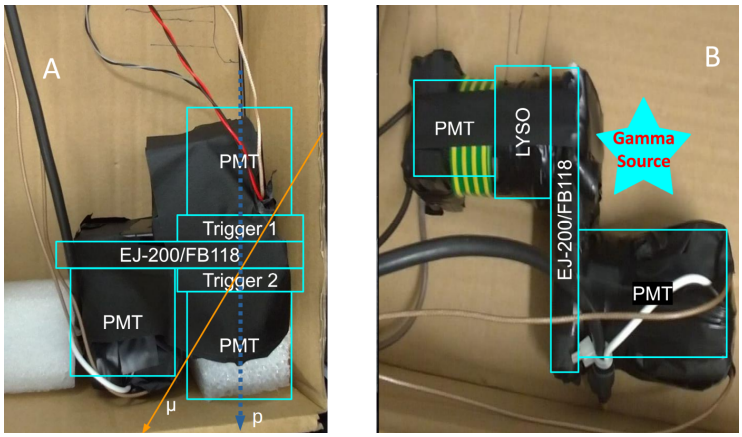

Figure 1. Photographs of the two test setups: (**A**) charged particle setup; (**B**) gamma-ray setup.

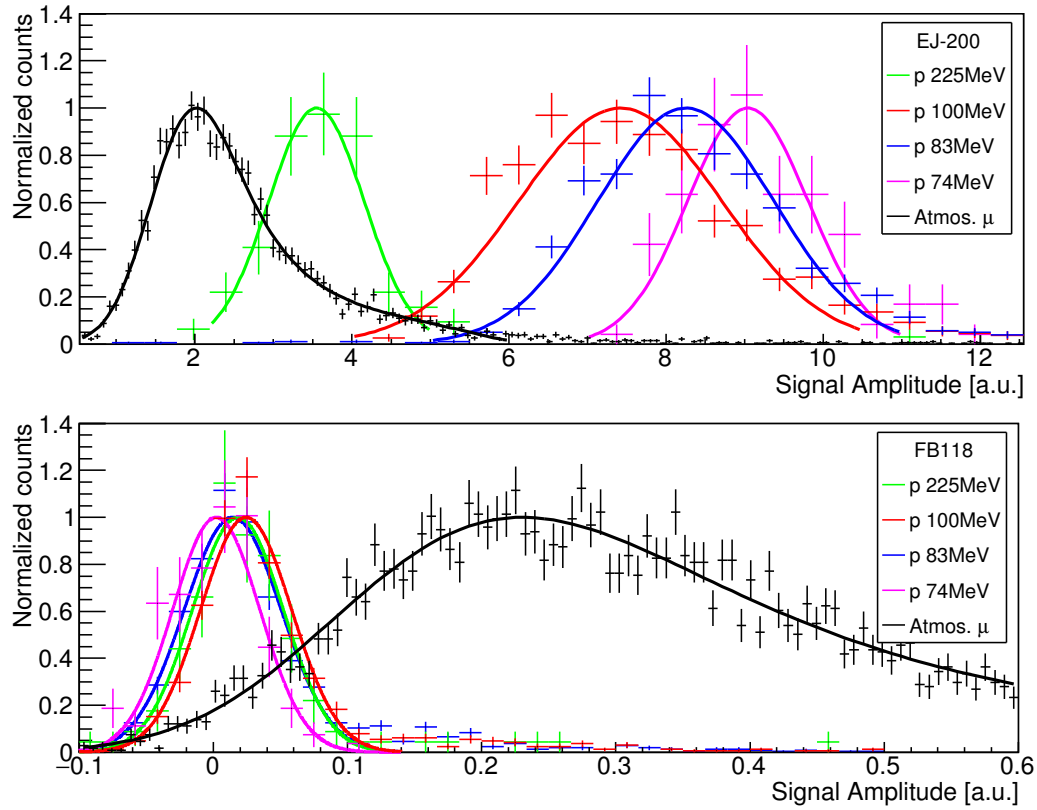

Figure 2. Amplitude distributions for protons and μ with EJ-200 (**top**) and FB118 (**bottom**). Continuous lines are Landau/Gaussian fitting functions to determine MPV values.

Table 1. MPVs of signal amplitudes for protons and μ in EJ-200 and FB118.

Particle	***p* 74 MeV**	***p* 83 MeV**	***p* 100 MeV**	***p* 225 MeV**	**μ**
MPV EJ-200	9.04 ± 0.08	8.25 ± 0.04	7.42 ± 0.05	3.55 ± 0.06	2.0 ± 0.1
MPV FB118	0.001 ± 0.003	0.014 ± 0.001	0.024 ± 0.001	0.018 ± 0.003	0.22 ± 0.01

The gamma-ray setup (Figure 1B) employed an 8 g LYSO crystal as a source of gamma rays from the internal ^{176}Lu radioactivity (mainly 202, 307, and 401 keV). Coincidences between LYSO and the FB118/EJ-200 samples were used as triggers. Additional measurements were performed using an external ^{60}Co source, which provides 1173 and 1332 keV γ rays. Due to the low atomic numbers of both plastics, only Compton recoils contribute to the signal, producing continuous spectra. The LYSO source mainly generates sub-threshold

electrons (the Cherenkov threshold for electrons in FB118 is ∼170 keV), whereas ^{60}Co generates a larger fraction of above-threshold electrons.

Figure 3 confirms that FB118 responds more strongly to the higher-energy Compton electrons from ^{60}Co, consistent with Cherenkov emission being dominant.

By comparing EJ-200 signal amplitude distributions with the FB118 ones, the ^{60}Co data constrain the residual scintillation yield of FB118 to be less than 10% of that of EJ-200. The LYSO test suggests it is up to 30 times lower, while proton-beam data indicate a fraction below 0.3%.

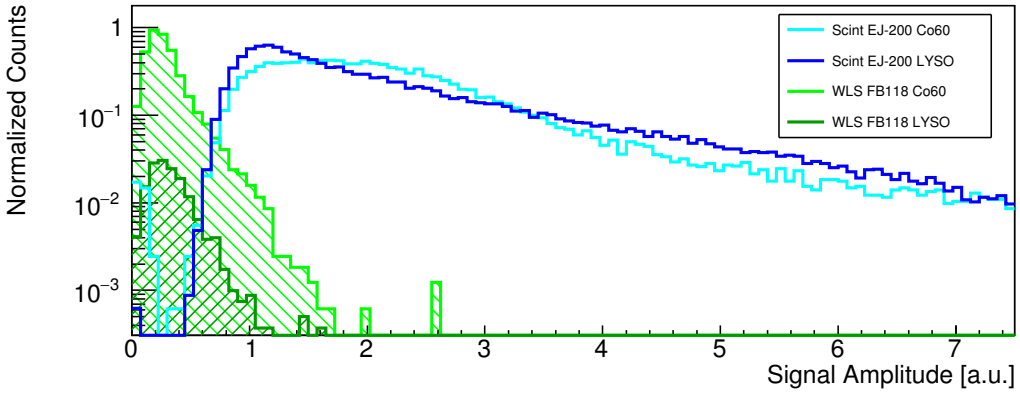

Figure 3. Gamma-ray signal amplitude distributions. FB118 (shaded) shows a significantly reduced response compared to EJ-200 (empty).

Using the known EJ-200 light yield (∼10,000 photons/MeV), the μ-test results indicate that FB118 produces ∼200 visible photons/mm via Cherenkov radiation. This notably high yield likely arises from FB118's capability to absorb UV photons and re-emit them efficiently in the visible range.

3. Test of Velocity Measurement with FB118

The capability of FB118 to measure the particle velocity thanks to Cherenkov emission was tested. In particular, we implemented a Time-of-Flight (ToF) detector using six layers of EJ-200 scintillators (30 × 25 × 1 cm^3): three layers placed on the floor and three on the roof, separated vertically by 5.1 m (see Figure 4).

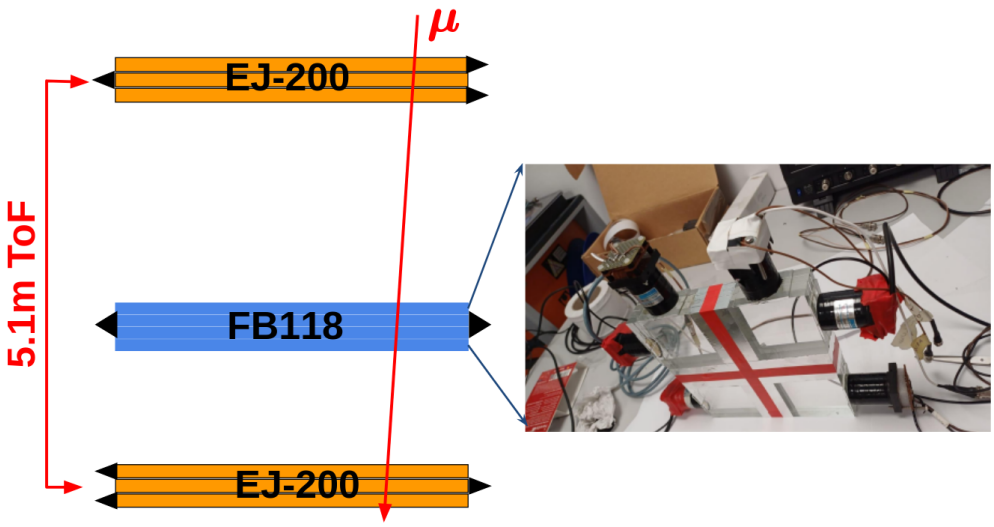

Figure 4. Schematic of the Time-of-Flight system used to compare the velocity measured via FB118 Cherenkov light emission with that obtained directly from the time delay between the top and bottom EJ-200 scintillator layers.

The data acquisition system, based on a CAEN DT5742 5 GS/s Switched Capacitor Digitizer, allowed measurement of the inverse particle velocity $1/\beta_{\mathrm{ToF}}$ with a resolution of about 8%. This resolution was dominated by variations in the propagation time of scintillation light within the EJ-200 pads, induced by the random impact position of the particles.

In the middle of the ToF system, we placed a Cherenkov detector based on FB118 (see inset of Figure 4). The detector was assembled by stacking four FB118 layers ($24 \times 24 \times 1$ cm^3) and coupling them to six Hamamatsu R5946 PMTs. The system was installed indoors and recorded 11.3k triggers, mostly from relativistic atmospheric muons. The $1/\beta_{\mathrm{ToF}}$ measurement identified a $\sim$2% fraction of slow, sub-threshold particles.

Figure 5a shows the average signal amplitude from the EJ-200 scintillator pads as a function of $1/\beta_{\mathrm{ToF}}$. The continuous black line represents the expected trend from the velocity dependence of the Bethe–Bloch energy-loss formula. Figure 5b reports the average Cherenkov signal amplitude from FB118, with the continuous line showing the expectation from the Frank–Tamm relation (Equation (2)). As expected, no Cherenkov signal is observed for slow particles ($1/\beta_{\mathrm{ToF}} > 1/\beta_{\mathrm{thr}} = \eta$, vertical dashed line).

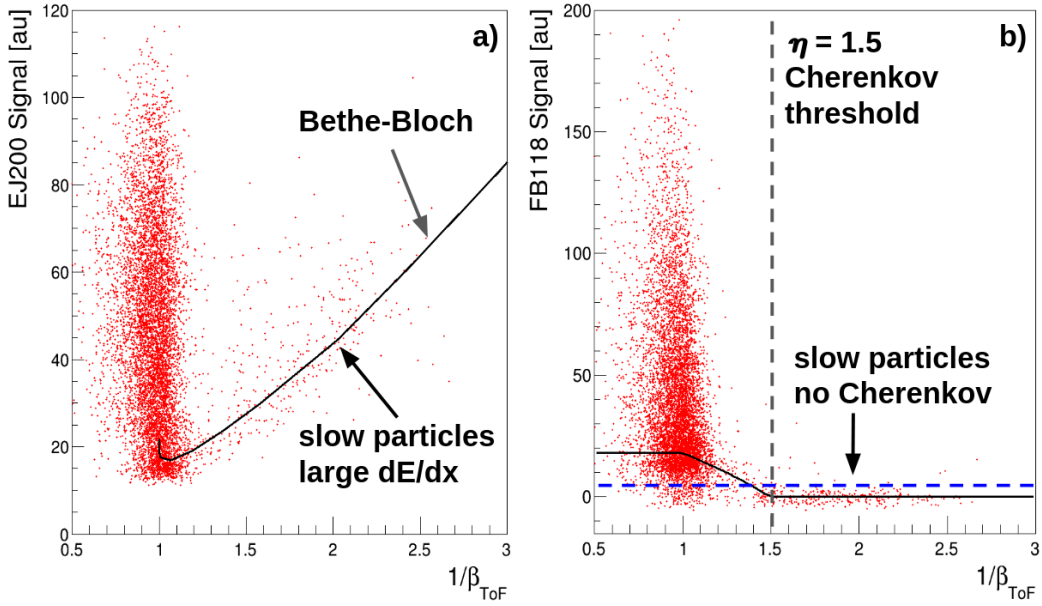

Figure 5. (**a**) Amplitude of the scintillation signal from EJ-200 as a function of inverse particle velocity measured via ToF. The continuous line shows the Bethe–Bloch expectation. (**b**) Amplitude of the Cherenkov signal from FB118. The continuous line shows the Frank–Tamm prediction. No Cherenkov signal is observed for particles slower than the threshold ($1/\beta_{\mathrm{thr}} = \eta$, vertical dashed line).

Figure 5 also illustrates the potential of a high-efficiency Cherenkov radiator such as FB118 for use in compact detectors for astroparticle physics. In particular, ToF detectors are typically excluded from most astroparticle experiments due to stringent requirements on compactness and power consumption. When relying solely on scintillator signals, slow particles are difficult to distinguish from the Landau tail generated by the dominant flux of fast particles, as illustrated in Figure 5a. In contrast, the horizontal dashed blue line in Figure 5b shows that a selection based on the Cherenkov signal is highly effective in identifying slow particles.

This is summarized in the left panel of Figure 6, where the selection of FB118 signals below 0.25 of the saturation level (red-filled histogram) efficiently identifies slow particles, with only a small contamination ($\sim$1.5%) from relativistic (MIP) events. This selection corresponds to $\beta < 0.7$, which, for protons, identifies kinetic energies below 400 MeV. Such a capability, achievable including an FB118 layer, would be of great interest for compact

experiments such as NUSES/Zirè [12], enabling simple electron–hadron separation in cosmic rays.

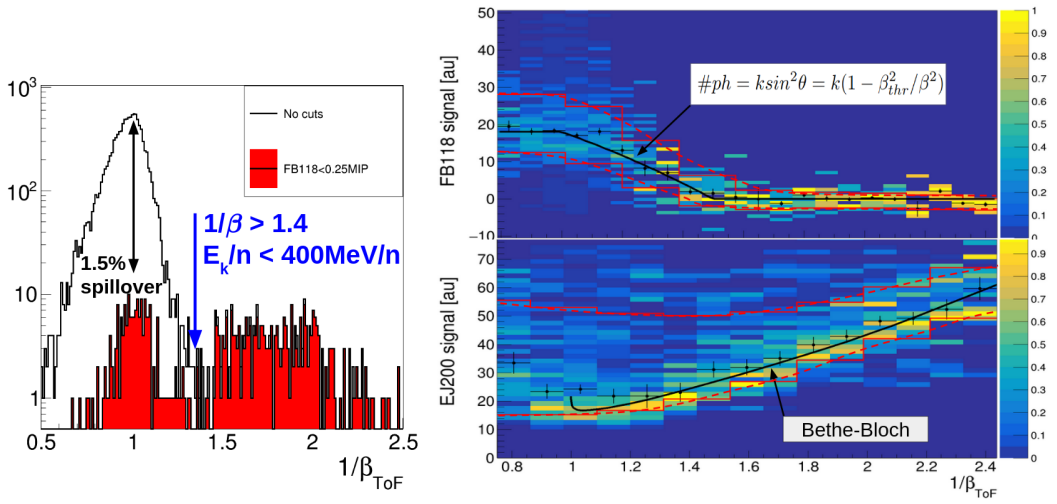

Figure 6. Performance of FB118 velocity measurements. (**Left**) Selection of FB118 signals below 0.25 of the saturation (MIP) level identifies mainly slow particles (red-filled). (**Right**) Signal distributions normalized in slices of $1/\beta_{ToF}$; red lines define the 68% signal amplitude probability contours. (**Right, top panel**) Velocity dependence of FB118 signal follows Frank–Tamm prediction. (**Right, bottom panel**) Velocity dependence of EJ-200 scintillation signal follows Bethe–Bloch prediction. Combining the complementary information from the two detectors allows a measurement of particle velocity with ∼20% resolution, without the need for a ToF system.

Similarly, future large-scale experiments proposed to identify stopping antinuclei in cosmic rays [13] will face relatively high trigger rates due to relativistic cosmic-ray protons and electrons. Using FB118 as a veto to select slow particles at trigger level could reduce this rate by about one order of magnitude.

Finally, the Bethe–Bloch relation allows the determination of particle velocity in the non-relativistic regime ($\beta < 0.7$) from energy-loss measurements in scintillator or silicon layers. This is shown in the bottom-right panel of Figure 6, where the normalized EJ-200 scintillation signal is plotted as a function of particle velocity. Complementarily, the amplitude distribution of the FB118 Cherenkov signal enables velocity measurements in the relativistic regime ($\beta > 0.7$), as seen in the top-right panel of Figure 6. Combining these two techniques, it is possible to achieve a velocity resolution better than 20%, making it possible to replace a full ToF system in many compact space detector designs.

4. Conclusions

We have characterized the optical response of the FB118 wavelength shifter, developed by "Glass to Power" [10]. No evidence of residual scintillation emission was found (less than 30 ph./MeV), fulfilling a key requirement for its integration into the PHeSCAMI detector [8,9,13].

In contrast, a strong Cherenkov emission (∼200 ph./mm) was observed, enhanced by the material's high UV-to-visible conversion efficiency. Therefore, the FB118 material is interesting as a compact Cherenkov radiator for particles in the velocity range $0.7 \lesssim \beta \lesssim 0.9$, particularly in small, space-based detectors where conventional Time-of-Flight systems are impractical.

Currently we are planning the development of aerogel (AGL) radiators ($\eta_{AGL} \sim 1.05$) doped with WLS fluors in our INFN/TIFPA laboratories. The relatively high threshold of AGL ($E_K > 2$ GeV for protons) will be useful to reduce the trigger rate of future large-scale spectrometers such as ALADInO [14].

Author Contributions: Conceptualization, F.N., L.E.G., R.N. and F.M.; methodology, L.E.G., R.N. and F.N.; software, L.E.G. and F.N.; validation, L.E.G., F.N. and R.N.; formal analysis, F.N. and L.E.G.; investigation, F.N., L.E.G. and E.V.; resources, D.C., F.B. and F.M.; data curation, L.E.G. and F.N.; writing—original draft preparation, F.N., L.E.G., R.N., F.B., D.C., F.M., L.R., P.S., E.V. and P.Z.; writing—review and editing, F.N., L.E.G., R.N., F.B., D.C., F.M., L.R., P.S., E.V. and P.Z.; visualization, L.E.G.; supervision, F.N. and P.Z.; project administration, F.N. and P.Z.; funding acquisition, F.N., L.R., P.S., E.V. and P.Z. All authors have read and agreed to the published version of the manuscript.

Funding: This work was supported by the Italian PRIN-2022 grant n. 2022LLCPMH "PHeSCAMI—Pressurized Helium Scintillating Calorimeter for AntiMatter Identification," CUP E53D23002100006.

Data Availability Statement: Data available upon request.

Acknowledgments: We thank A. Pavlovic for providing the FB118 samples.

Conflicts of Interest: Author F.B. has received research grants from Company "Glass to Power". The Company "Glass to Power" had no role in the design of the study; in the collection, analyses, or interpretation of data; in the writing of the manuscript, and in the decision to publish the results.

Abbreviations

The following abbreviations are used in this manuscript:

MIP	Minimum Ionizing Particle
PMT	Photomultiplier Tube
ToF	Time-of-Flight
UV	Ultraviolet
WLS	Wavelength Shifter

References

1. Badino, G.; Galeotti, P.; Periale, L.; Saavedra, O.; Turtelli, A. The effect of wavelength shifters on water cherenkov detectors. *Nucl. Instrum. Methods Phys. Res.* **1981**, *185*, 587–589. [CrossRef]
2. Krider, E.; Jacobson, V.; Pifer, A.; Polakos, P.; Kurz, R. Wavelength-shifted Cherenkov radiators. *Nucl. Instrum. Methods* **1976**, *134*, 495–503. [CrossRef]
3. Grande, M.; Moss, G.R. An optimised thin film wavelength shifting coating for Cherenkov detection. *Nucl. Instrum. Methods Phys. Res.* **1983**, *215*, 539–548. [CrossRef]
4. Claus, R.; Seidel, S.; Sulak, L.; Bionta, R.M.; Blewitt, G.; Bratton, C.; Casper, D.; Ciocio, A.; Dye, S.; Errede, S.; et al. A waveshifter light collector for a water Cherenkov detector. *Nucl. Instrum. Methods Phys. Res. Sect. A Accel. Spectrometers Detect. Assoc. Equip.* **1987**, *261*, 540–542. [CrossRef]
5. Murphy, R.; Binns, W.; Bose, R.; Brandt, T.; Braun, D.; Daniels, W.; De Nolfo, G.; Dowkontt, P.; Fitzsimmons, S.; Hahne, D.; et al. In-flight Performance of the Super-TIGER Cherenkov Counters. In Proceedings of the 33rd International Cosmic Rays Conference, ICRC 2013, Sociedade Brasileira de Fisica, Rio de Janeiro, Brazil, 2–9 July 2013.
6. Eljen Technology. Wavelength Shifting Plastics: EJ-280, EJ-282, EJ-284, EJ-286. 2024. Available online: https://eljentechnology.com/products/wavelength-shifting-plastics/ej-280-ej-282-ej-284-ej-286 (accessed on 19 July 2025).
7. Brizzolari, C.; Brovelli, S.; Bruni, F.; Carniti, P.; Cattadori, C.; Falcone, A.; Gotti, C.; Machado, A.; Meinardi, F.; Pessina, G.; et al. Enhancement of the X-Arapuca photon detection device for the DUNE experiment. *J. Instrum.* **2021**, *16*, P09027. [CrossRef]
8. Nozzoli, F.; Rashevskaya, I.; Ricci, L.; Rossi, F.; Spinnato, P.; Verroi, E.; Zuccon, P.; Giovanazzi, G. Antideuteron Identification in Space with Helium Calorimeter. *Instruments* **2024**, *8*, 3. [CrossRef]
9. Ghezzer, L.E.; Giovanazzi, G.; Nozzoli, F.; Ricci, L.; Rossi, F.; Spinnato, P.; Verroi, E.; Zuccon, P.; Bruni, F.; Meinardi, F. Development of a Pressurized Helium Scintillating Calorimeter for AntiMatter Identification. *Proc. Sci.* **2025**, *EXA-LEAP2024*, 048. [CrossRef]
10. Glass to Power SpA. Wavelength Shifters—Nanotechnologies. 2024. Available online: https://www.glasstopower.com/wavelength-shifters/ (accessed on 19 July 2025).
11. Fourati, M.A.; Maris, T.; Skene, W.G.; Bazuin, C.G.; Prud'homme, R.E. Photophysical, Electrochemical and Crystallographic Investigations of the Fluorophore 2,5-Bis(5-tert-butyl-benzoxazol-2-yl)thiophene. *J. Phys. Chem. B* **2011**, *115*, 12362–12369. [CrossRef] [PubMed]
12. Panzarini, G.; Barbato, F.C.T.; De Mitri, I.; Di Giovanni, A.; Mazziotta, M.N.; Nicolaidis, R.; Nozzoli, F.; Pillera, R.; Savina, P. The Ziré instrument onboard the NUSES space mission. *Nucl. Instrum. Meth. A* **2024**, *1068*, 169794. [CrossRef]

13. Gezzer, L.E.; Nozzoli, F.; Ricci, L.; Verroi, E.; Spinnato, P.; Zuccon, P. Advancing Anti-Deuteron Detection in Cosmic Rays: Innovations in Methods and Technologies. *Proc. Sci.* **2025**, *ICRC2025*, 508.
14. Adriani, O.; Altomare, C.; Ambrosi, G.; Azzarello, P.; Barbato, F.C.T.; Battiston, R.; Baudouy, B.; Bergmann, B.; Berti, E.; Bertucci, B.; et al. Design of an Antimatter Large Acceptance Detector In Orbit (ALADInO). *Instruments* **2022**, *6*, 19. [CrossRef]